



New ceramic EPR resonators with high dielectric permittivity

Iryna Golovina^{a,1}, Ilia Geifman^{a,*}, Anatolii Belous^{b,2}

^a Institute of Semiconductor Physics of NASU, Pr. Nauki 41, Kiev 03028, Ukraine

^b Institute of General and Inorganic Chemistry of NASU, Academician Palladin Avenue 32-34, Kiev 03680, Ukraine

ARTICLE INFO

Article history:

Received 13 December 2007

Revised 15 July 2008

Available online 6 September 2008

Keywords:

Dielectric ceramic resonator
Electron paramagnetic resonance
Sensitivity

ABSTRACT

New EPR resonators were developed by using a ceramic material with a high dielectric constant, $\varepsilon = 160$. The resonators have a high quality factor, $Q = 10^3$, and enhance the sensitivity of an EPR spectrometer up to 170 times. Some advantages of the new ceramic resonators are: (1) cheaper synthesis and simplified fabricating technology; (2) wider temperature range; and (3) ease of use. The ceramic material is produced with a titanate of complex oxides of rare-earth and alkaline metals, and has a perovskite type structure. The resonators were tested with X-band EPR spectrometers with cylindrical (TE_{011}) and rectangular (TE_{102}) cavities at 300 and 77 K. We discovered that EPR signal strength enhancement depends on the dielectric constant of the material, resonator geometry and the size of the sample. Also, an unusual resonant mode was found in the dielectric resonator-metallic cavity structure. In this mode, the directions of microwave magnetic fields of the coupled resonators are opposite and the resonant frequency of the structure is higher than the frequency of empty metallic cavity.

© 2008 Elsevier Inc. All rights reserved.

1. Introduction

Applications of the electron paramagnetic resonance (EPR) method have been developing intensively in biology and medicine where samples are not specially doped with a paramagnetic impurity and contain natural amounts of paramagnetic centers such as radicals or transition metals [1]. Because the samples are often tissues or blood samples from animals or humans and are usually very limited in size, increasing EPR spectrometer sensitivity is extremely important. Successful increase of sensitivity is achieved as a result of constant developments of new resonator designs. The present work is devoted to the development of a group of dielectric resonators, which have essential advantages when compared to metallic cavities normally used in EPR. Some advantages of a dielectric resonator (DR) in comparison to a standard metallic cavity are: (1) smaller size; (2) greater filling factor; (3) greater magnetic field on a sample; and (4) smaller cost. Metallic cavities cost more because they involve the labor-intensive processing of the surface and additional drawing on the internal surface of a gold film or other conductivity-improving material.

The original idea of using a DR in EPR spectroscopy is attributed to Rosenbaum [2]. His resonator was made of a material

with the dielectric constant $\varepsilon = 10$. Walsh and Rupp [3] made a fully-functional DR with which they have replaced the metallic cavity in an EPR spectrometer. This DR was made of ceramics with $\varepsilon = 29$, had a quality factor $Q = 6000$, and resulted in a 30-fold increase of the EPR signal. The disadvantages were the limited efficiency due to the low dielectric permittivity, and the labor-intensive process that included developing a special coupling system with a waveguide path, a shield, creating modulation, etc. In the same year [4] another dielectric resonator was developed, made of ceramics with a dielectric constant of 38 and a quality factor of $Q = 5600$, which allowed an increase in signal strength of a factor close to 100. This resonator was used in with a small temperature range, from -50 up to $+50$ °C, and was inconvenient for similar reasons to Walsh and Rupp's resonator [3]. Wolak and Hilczner [5] also replaced a standard metallic cavity with a ceramic resonator of $\varepsilon = 10$ in laboratory EPR measurements. Double-stacked DR made of ceramics with $\varepsilon \approx 30$ was tested by Sienkiewicz et al. [6] and by Jaworski et al. [7]. The line intensity observed for the double DR was about 30 times larger than that obtained in the rectangular (TE_{102}) metallic cavity [7]. Doubly stacked DR was mounted on Bruker ER-200 D EPR spectrometer replacing a standard metallic cavity. Thus, a coupling device, shield and support structure needed to be designed for that DR-based system. The authors [8–10] simplified the DR coupling and shielding problems by placing a DR inside a metallic cavity.

Recently, ferroelectric resonators have been developed and their properties were investigated in detail [11–15]. These resonators were made of single crystals of potassium tantalite (which is a virtual ferroelectric) and had a dielectric constant of 261 at room

* Corresponding author. Present address: 10353 Dearlove Road #3D, Glenview, IL 60025, USA. Tel.: +1 847 298 1347; fax: +1 847 718 1149.

E-mail addresses: golovina@isp.kiev.ua (I. Golovina), geifmani@yahoo.com (I. Geifman), belous@ionc.kar.net (A. Belous).

¹ Tel.: +38 044 525 8582, +38 044 540 4746.

² Tel.: +38 044 424 2211.

temperature and 4000 at 4.2 K. A feature of this material is that its dielectric losses decrease as dielectric constant increases [16]. At room temperature, the quality factor of these resonators is 10,000. Resonators with various geometries have been made and tested. They provided an amplification of the EPR signal by a factor of 50–100. Most of these resonators were placed in the middle of the metallic cavity [11–14] therefore additions for its excitation and adjustment were not required. This is an essential advantage. However, the temperature range application of these resonators has been very limited because of the strong temperature dependence of their dielectric constant. Also, as calculations have shown [17] at helium temperatures the thickness of walls became so thin (0.2–0.5 μm) that it appeared physically impossible to make such a resonator for low-temperature experiments. Growth of a single crystal requires significant energy and time resources; additional processing is often required to obtain the necessary size and shape of the resonator. We therefore tackled a problem of how to: (1) receive higher sensitivity, (2) produce the resonator by simplified and less expensive technology, and (3) expand the functional temperature range of the resonator.

2. Methods

2.1. Resonator material

DRs were made of the ceramic material composed of strontium and calcium titanates, which are crystallized in the perovskite type structure [18]. Oxides of zinc, aluminium and rare-earth metals were also added in order to decrease the sintering temperature and increase the quality factor.

The ceramics were made by solid-state synthesis at a sintering temperature of 1350 °C for 2–3 h. Cylindrical and rectangular compression molds of the necessary sizes were used so no additional machining was necessary. The basic dielectric characteristics of the ceramics were: the dielectric constant ϵ was 160, the temperature change factor of ϵ ($\text{TC}\epsilon$) was about 10^{-5} (700 ppm/K); the dielectric losses ($\tan\delta$) at frequency of 10 GHz was 10^{-3} . In Table 1 the characteristics of three most typical ceramic resonators are presented. The resonator DR1 with $\epsilon = 35$ was taken for comparison. Two resonators DR2 and DR3 of rectangular and cylindrical symmetry were made of ceramics with a high value of ϵ , to determine which symmetry is more effective. In addition, the sizes of these resonators and dielectric characteristics of ceramics are shown. All resonators have a through hole for input of a capillary with the sample.

2.2. Calculation technique

The main microwave characteristics of resonators, their own resonant frequency and the corresponding resonant sizes were computed using a commercially available computer package Ansoft High Frequency Structure Simulator (Ansoft HFSS v.10, Pittsburgh, PA, USA). This program was also used for the finite-element simulations of electromagnetic fields inside the developed resonators. The program provides “eigenmode” and “driven mode” solutions of Maxwell’s equations. In this work, only “eigenmode” solutions were used.

2.3. Experimental details

Estimation of a dielectric constant (ϵ) of the ceramic material used was carried out within wide frequency range (1–10 MHz) on Q-meter M560 (made in Czechoslovakia). Further details of the measurements are described elsewhere [19–22].

Note that this material has no dispersion, i.e. its dielectric constant is not a function of frequency.

Measurements of microwave characteristics (resonant frequency and a quality factor) of the DRs were performed using an Agilent #5230A PNA-L Network Analyzer. It was employed a hollow cylindrical cavity of 38-mm diameter and 20-mm height, internal surface of which is silver-plated. A DR was inserted inside the cavity, in which the input is connected through a coaxial transmission line. By adjusting the coupling, a symmetrical S_{11} amplitude plot should be achieved. Then, the resonant frequency (f_0) is taken. A quality factor (Q) is inversely proportional to the difference between the 3-dB frequencies f_1 and f_2 at each side of the resonance and determined as $Q = f_0/(f_1 - f_2)$. Q -factor measurement procedure with network analyzer is well developed and described by Darko Kajfez [23].

EPR experiments were performed on X-band CW EPR spectrometers RE 1307 (with cylindrical TE_{011} cavity) and Radiopan SE/X 2544 (with rectangular TE_{102} cavity) at room and liquid nitrogen temperatures. Spectrometer RE 1307 was designed by the Institute of Scientific Instrumentation of Academy of Sciences of the USSR and built in Chernogolovka plant, Moscow region, Russia. Spectrometer SE/X 2544 was produced by Radiopan company (Polish Academy of Sciences) in Poznan, Poland. As shown in Fig. 1, a DR was located in the middle of the metallic rectangular TE_{102} (or cylindrical TE_{011}) cavity in the maximum microwave magnetic field so that the axis of the DR was parallel to the microwave (MW) magnetic field and perpendicular to the DC magnetic field. Arrows schematically show the concentration of MW magnetic field (B_1) due to the presence of the DR. For experiments at 77 K standard quartz dewar (delivered with an EPR spectrometer) was used. To minimize the shift of the resonant frequency, a metal (cooper) stick was putted on the bottom of the quartz dewar. In order to avoid that tuning routine, the temperature below 300 K should be attained by nitrogen (or helium) vapor blowing. In such a case a liquid nitrogen (or helium) could be heated by an electric furnace controlled by temperature stabilizer. Moreover, vapor

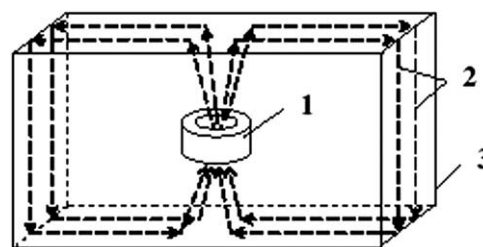


Fig. 1. A schematic representation of the DR- TE_{102} resonant structure: (1) a DR; (2) microwave magnetic field B_1 ; and (3) metallic TE_{102} cavity.

Table 1
Technical characteristics of the DRs

Resonator	Symmetry	Dimensions	ϵ	$\text{TC}\epsilon$ (K^{-1})	$\tan\delta_{10\text{GHz}}$
DR1	Cylindrical	OD = 5.4 mm, L = 2.5 mm, ID = 1.5 mm	35	10^{-7}	1.5×10^{-4}
DR2	Rectangular	$A = B = 3.1$ mm, $L = 1.1$ mm, ID = 1.1 mm	160	10^{-5}	10^{-3}
DR3	Cylindrical	OD = 2.9 mm, $L = 1.4$ mm, ID = 1.1 mm	160	10^{-5}	10^{-3}

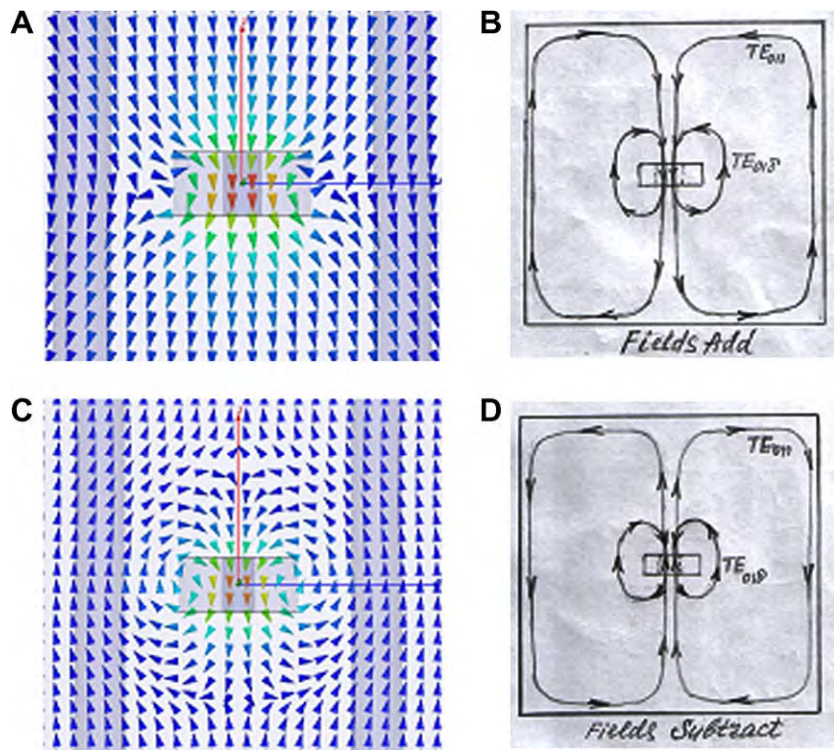


Fig. 2. Distributions of the MW magnetic fields inside a DR-TE₀₁₁ resonant structure in vector (A and C) and schematic (B and D) forms for two cases: (A and B) the fields are parallel; (C and D) the fields are opposite.

blowing procedure is better then usage of a quartz dewar, because it prevents boiling of liquid nitrogen. This leads to noise increasing and consequently decreases signal-to-noise ratio of EPR spectra.

A 2,2-diphenyl-1-picrylhydrazyl (DPPH) powder of 2-mm height and Mn(NO₃)₂ · 6H₂O solution of 4-mm height were used as samples. Each sample was located in a quartz capillary with an outer diameter (OD) of 1 mm.

3. Results and discussion

In Table 2 the calculated (f_{cal}) and experimental (f_{exp}) values of resonant frequencies of three DRs and the frequencies of resonant structures (when the DR is located in the metallic cavity) are presented.

An unusual change of f_{exp} occurred when a DR was placed into a metallic cavity. Normally, when a dielectric object is placed into a maximum MW magnetic field inside a metallic cavity, the frequency of the latter goes down. In our experiments we observed both an increase and decrease of frequency (see Table 2). The DR-metallic cavity resonant structure simulations show the appearance of the lowest modes, which are TE₀₁₁ mode in the

metallic cylindrical cavity and TE_{01,δ} mode in the DR, at two different frequencies. As shown in Fig. 2, the directions of the fields are: at lower frequency the directions of fields coincide, and at higher frequency they are opposite, i.e. at lower frequency the fields are additive, while at higher frequency they are subtractive in absolute value. The difference in the resulting value of magnetic field B_1 on a sample in these two cases is approximately 1.5 times. In the experiment, only one resonance is visible at any of these two frequencies depending on which gets in the working zone of MW generator. For example, in the case of resonator DR1, a resonance at a lower frequency is visible in the experiment. In cases of DR2 and DR3, however, resonances at higher frequencies are visible. This means that if the sizes of resonators DR2 and DR3 are slightly changed so that in the experiment we observe their resonance not at a higher frequency (as now), but at a lower frequency (when the fields are additive), we shall obtain a greater increase of the EPR signal.

The matching of resonant frequencies of the empty cavity TE₀₁₁ mode to TE_{01,δ} mode of the DR is also important. We have made the

Table 2
Microwave characteristics of the DRs and DR-cavity resonant structures

Resonator	f_{cal} (MHz)	f_{exp} (MHz)	DR-TE ₀₁₁		DR-TE ₁₀₂	
			f_{cal} (MHz)	f_{exp} (MHz)	f_{cal} (MHz)	f_{exp} (MHz)
Cavity	–	–	9400	9394	9408	9409
DR1	9918	10,178	9060	9099	9090	9164
			10,205		10,301	
DR2	8352	8581	8303		8324	
			9454	9458	9471	9473
DR3	8737	8992	8662		8678	
			9457	9471	9480	9478

Table 3
Calculated characteristics of the DRs and DR-TE₀₁₁ resonant structures

Resonator	Dimensions (mm ³)	f_{cal} (MHz)	DR-TE ₀₁₁		
			f_{str}^a (MHz)	I_{cal} (a.u.)	G
TE ₀₁₁	Standard cavity	9400	–	1.9	–
DR2	A = B = 3.1 mm, L = 1.1 mm, ID = 1.1 mm	8352	8303	34.4	18
			9454	15.7	8
DR2a	A = B = 2.66 mm, L = 1.1 mm, ID = 1.1 mm	9405	9187	42.7	23
			9621	40.1	21
DR3	OD = 2.9 mm, L = 1.4 mm, ID = 1.1 mm	8737	8662	45.9	24
			9457	26.3	14
DR3a	OD = 2.65 mm, L = 1.4 mm, ID = 1.1 mm	9416	9203	50.9	27
			9612	48.1	25

^a f_{str} denotes calculated resonant frequency of DR-TE₀₁₁ structure.

elaboration (article based on the results of this study is under preparation) that the best improvement in EPR signal strength is achieved when resonant frequencies of the $TE_{01\delta}$ mode of the DR is fully matched to empty TE_{011} mode. To demonstrate that, modeling calculations have been made. First, we changed the dimensions of resonators DR2 and DR3 so, that its own resonant frequency (f_{cal}) becomes very close to the frequency of TE_{011} cavity. Then, signal intensity (I_{cal}) and G factor for each case were calculated by using Ansoft HFSS program. The results are summarized in Table 3, in which resonators DR2a and DR3a denote the model resonators with changed dimensions. In calculations solid dielectric sample of ZnS ($\epsilon = 8.9$, $\tan\delta = 0.0019$) with sizes $0.4 \times 0.4 \times 2.8 \text{ mm}^3$ was used. It should be noted that in Table 3 only a lower frequency of DR–cavity resonant structure, i.e. when the fields of TE_{011} and $TE_{01\delta}$ modes are additive, is presented.

In Figs. 3 and 4 the EPR spectra of DPPH and $Mn(NO_3)_2 \cdot 6H_2O$ samples, respectively, are placed into an empty rectangular TE_{102} metallic cavity and into the resonant structures with resonators DR1, DR2 and DR3. Essentially the intensity of EPR signal increases in resonant structures with DRs compared to a metallic cavity. It should be noted that only the $+1/2 \leftrightarrow -1/2$ fine transition is visible in the EPR spectra of Mn^{2+} (see Fig. 4) in disordered systems, such as powders, glasses, thin films, solutions, etc. [24,25]. Moreover, because of the high concentration of manganese in $Mn(NO_3)_2 \cdot 6H_2O$ solution, six lines of hyperfine structure of Mn^{2+} ions ($I = 5/2$) are broadened due to dipole–dipole interactions. Similar spectra were observed for both samples with DRs placed in a cylindrical metallic cavity. Also, EPR spectra of the above samples were

recorded at 77 K with all three DRs each placed into a TE_{102} cavity. In this case, the frequency (f_{exp}) of the DR–metallic cavity resonant structure should be tuned to the value it had at room-temperature experiments (see Table 2), in order to get the same gain factor (G). Note that G denotes the ratio between the signal intensity obtained in the DR–metallic cavity resonant structure and in the metallic cavity alone at the same incident MW power, modulation amplitude, receiver gain, time constant and temperature.

In Table 4 the gain factors (G) computed for each sample and for both metallic cavities, cylindrical and rectangular, are summarized. As apparent in Table 4, G values obtained from experiments in the cylindrical (TE_{011}) cavity are approximately two times less than that in the rectangular (TE_{102}) cavity. There is a possible connection to the distinction in quality factors of cylindrical and rectangular metallic cavities. Normally, a cylindrical metallic cavity has almost twice the quality than a rectangular one. We obtained a greater G value in the rectangular cavity when the initial signal is less. This is essential for EPR spectrometers equipped with rectangular metallic cavity. Also, it is possible to see that the G values of the rectangular ceramic resonator (DR2) are lower than that of the cylindrical ceramic resonator (DR3). Finally, it should be noted that an increase of signal strength for the $Mn(NO_3)_2 \cdot 6H_2O$ sample is less than that for the DPPH sample because of different sample height: the solvent sample has a height of 4 mm, while the powder sample has a height of 2 mm. This means that due to the field B_1 concentration there was an increase of signal for only part of the sample, which was located inside the DR. The other part of sample (practically half the height) is located outside of the DR so it does not have

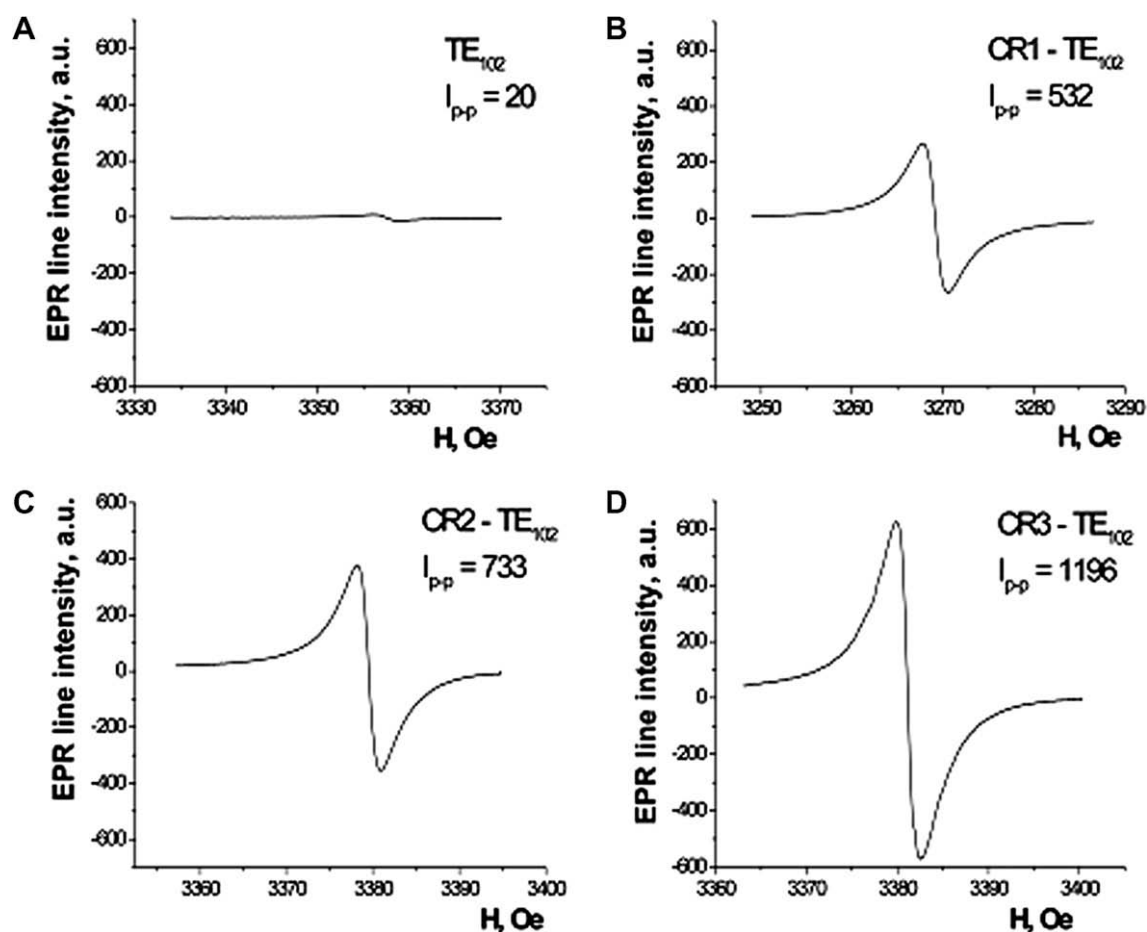


Fig. 3. EPR signals of DPPH sample placed into empty TE_{102} cavity (A) and into resonant structures with DR1 (B), DR2 (C) and DR3 (D). All spectra were recorded at room temperature, incident MW power $P = 1 \text{ mW}$ and modulation amplitude 0.2 Oe .

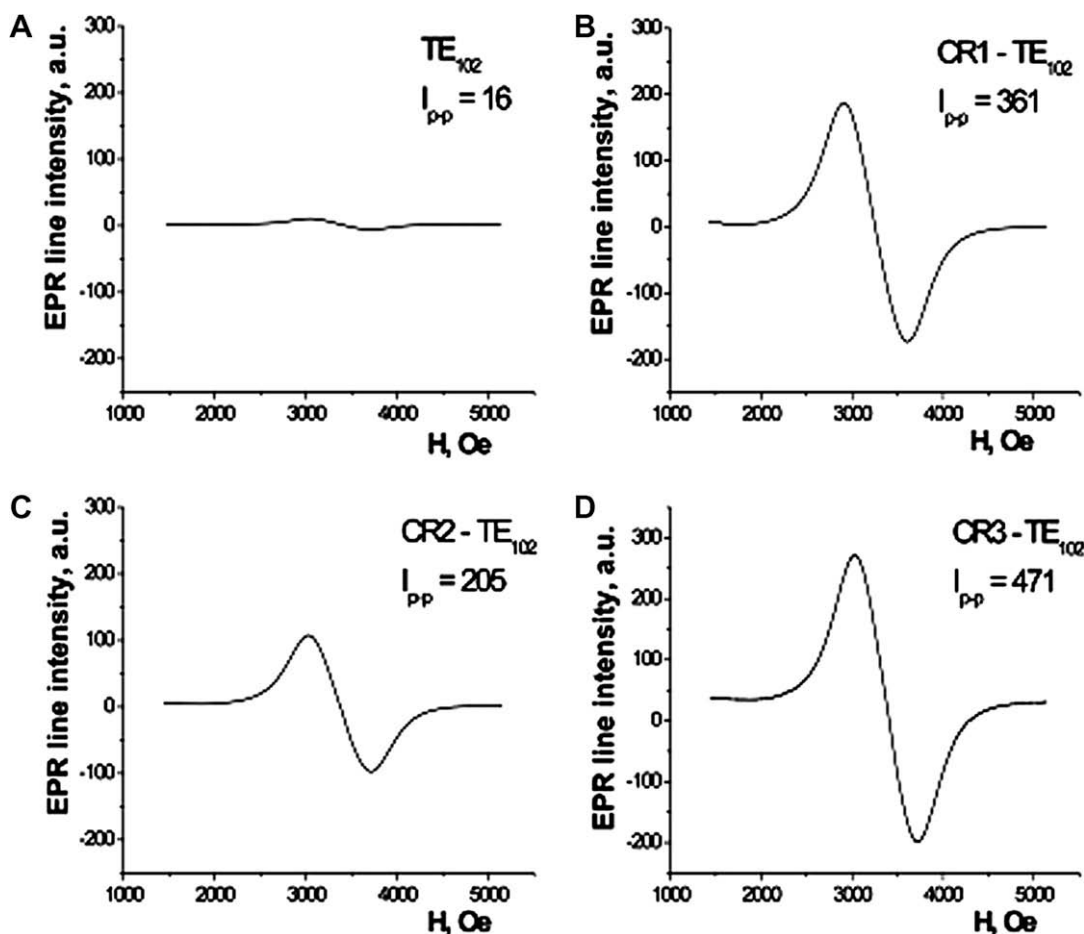


Fig. 4. EPR signals of $\text{Mn}(\text{NO}_3)_2 \cdot 6\text{H}_2\text{O}$ sample placed into empty TE_{102} cavity (A) and into resonant structures with DR1 (B), DR2 (C) and DR3 (D). All spectra were recorded at room temperature, incident MW power $P = 3$ mW and modulation amplitude 2 Oe.

Table 4

Summarized G values for DPPH and $\text{Mn}(\text{NO}_3)_2 \cdot 6\text{H}_2\text{O}$ samples placed into different resonant structures

Resonator	DPPH		$\text{Mn}(\text{NO}_3)_2 \cdot 6\text{H}_2\text{O}$	
	DR- TE_{011} ($P^a = 1$ mW)	DR- TE_{102} ($P^a = 1$ mW)	DR- TE_{011} ($P^a = 3.16$ mW)	DR- TE_{102} ($P^a = 3.16$ mW)
DR1	12	26	10	22
DR2	15	36	8	15
DR3	25	59	13	29

^a P denotes incident microwave power.

the increased field value and as a result the G value, turns out almost two times less. This result allows us to conclude that to obtain the greatest gain factor the optimum sample height should be equal to or less than a height of the DR.

We also carried out the experiments at various incident MW power with the same two samples and with two cylindrical ceramic resonators DR1 and DR3 placed into metallic TE_{102} cavity. EPR spectra were recorded at room temperature. It is known that for non-saturable samples, EPR line intensity (I) is proportional to a square root from incident MW power (P), i.e. $I \sim P^{1/2}$. Fig. 5 shows the results obtained with the $\text{Mn}(\text{NO}_3)_2 \cdot 6\text{H}_2\text{O}$ sample. The width of EPR line remains constant, and peak-to-peak intensity (I_{p-p}) is presented here. In Fig. 5A the points are experimental values and a dashed line represents theoretically calculated values according to the above relation. Agreement between theory and experiment shows that the given sample is nonsaturable. Fig. 5B

demonstrates the values of the gain factor (G) reported in accordance with the experimental data presented in Fig. 5A. Apparently (within the limits of 5% error) factor G is almost constant. The situation changes, however, when the sample is saturable. In Fig. 6A the dependence of integrated intensity versus incident MW power obtained with the DPPH sample is presented. Note that unlike the previous sample, here the width and the form of EPR line varied as power increased presenting an integrated intensity. As seen from Fig. 6A, there is a deviation of experimental points from a theoretical dashed line above 30 mW for both DRs, indicating a saturation of the sample. In Fig. 6B the dependence of factor G on incident power P for this sample is shown. The gain factor decreases as power increases for both DRs, although the decrease is slower for DR1 than for DR3. This indicates that for saturable samples it would be much more effective to carry out the experiments at the lowest incident MW power. This is an important result, especially for EPR spectrometers where normally saturable biological objects are investigated. Additionally, the use of the DR will make possible the replacement of expensive 1-kW amplifiers used in pulsed EPR spectrometers with cheaper 1-W or 10-W amplifiers. For instance, high-permittivity SrTiO_3 dielectric resonator has already made it possible to use solid-state amplifier with output power of about 1 W in certain pulsed EPR applications [26].

To estimate the spin number sensitivity, a model experiment was performed. It is known, that integral intensity of absorption EPR line (A) corresponds to the number of spins (N) in the sample [27]. In case of the first-derivative absorption EPR line (suppose the line is symmetrical), an integral intensity A is proportional to

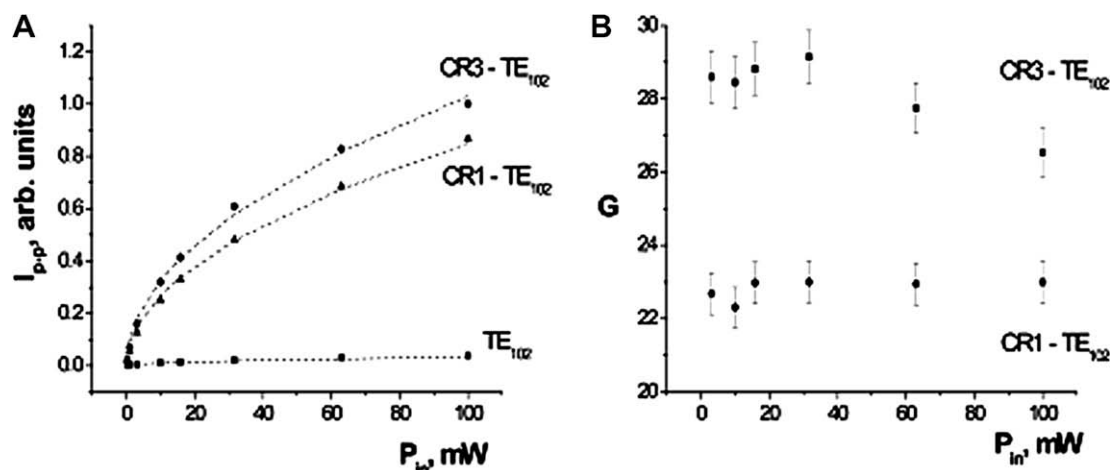


Fig. 5. Signal peak-to-peak intensity (A) and gain factor (B) versus incident MW power for $\text{Mn}(\text{NO}_3)_2 \cdot 6\text{H}_2\text{O}$ sample.

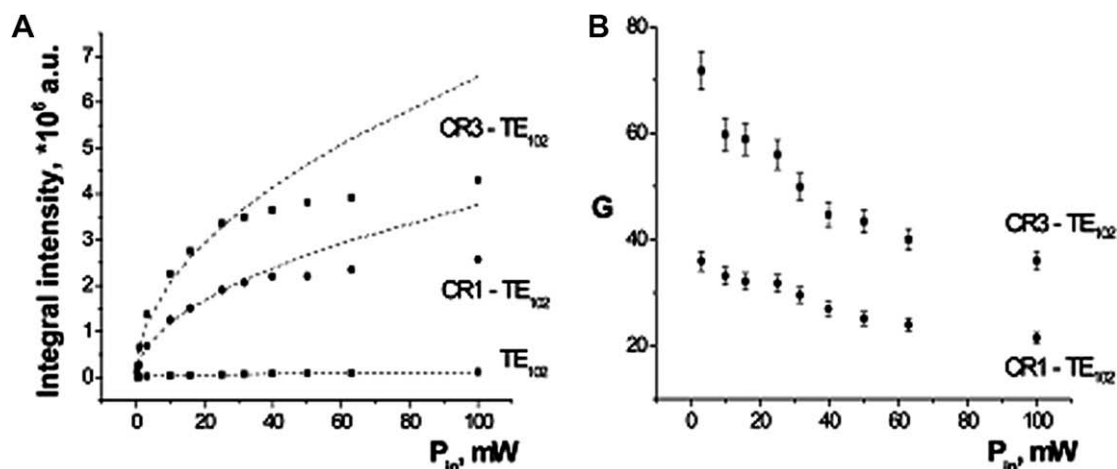


Fig. 6. Integral intensity (A) and gain factor (B) versus incident MW power for DPPH sample.

$I_{p-p} \cdot \Delta H_{p-p}^2$, where ΔH_{p-p} is peak-to-peak linewidth. Consider two point samples of DPPH with different number of spin N_1 and N_2 . If modulation amplitude is much less than the linewidth, so that ΔH_{p-p} remains unchanged, then the ratio of EPR line intensities of the samples I_{p-p1}/I_{p-p2} will be equal to the ratio N_1/N_2 . In terms of sensitivity, line intensity should be replaced by signal-to-noise ratio (SNR). Now, if modulation amplitude reduces 10 times, that will be identically to the detecting the sample with 10-times smaller number of spins. For such an experiment a point DPPH sample (1.5×10^{13} spins/G) in capillary of 0.8 mm inner diameter (ID) and a ceramic resonator DR2 were used. With this sample in DR-TE₁₀₂ structure, SNR = 5:1 was obtained at modulation amplitude 0.125×10^{-2} G, incident MW power 10 mW, time constant 0.3 s, scan time 60 s, without accumulation (Fig. 7A). With the same sample in TE₁₀₂ cavity alone, SNR = 3:1 was obtained at modulation amplitude 0.125 G under above incident power, time constant and scan time (Fig. 7B). Then, to obtain SNR = 3:1 at the latter conditions in DR-TE₁₀₂ structure, spin number in the sample should be reduced by a factor of about 170. Thus, using Radiopan SE/X 2544 spectrometer and DR-TE₁₀₂ resonant structure, spin number of 8.8×10^{10} spins/G could be detected with SNR = 3:1 at modulation amplitude 0.125 G, incident MW power 10 mW, time constant 0.3 s, scan time 60 s, without accumulation. Taking into account that theoretically evaluated spin number sensitivity of Radiopan SE/X 2544 spectrometer is 5×10^{10} spins/G, the usage of the ceramic resonator with $\epsilon = 160$ can improve the sensitivity approxi-

mately to 5×10^8 spins/G. Analogical experiment was performed at 77 K (Fig. 8). Note that in low-temperature experiment the DR with the sample were placed in a quartz dewar (see Section 2.3). Due to frequency shift and nitrogen boiling, G factor becomes about 50 that smaller compared to 170 in room-temperature experiment. It should be noted that the G factors are true only if sample volume is limited.

Existence of spurious EPR signals arising from impurities is the disadvantage of the DRs compared to the standard EPR cavities. To provide a clear picture, the background spectra recorded at room and liquid nitrogen temperatures are depicted in Fig. 9. As shown by modeling experiment with a point DPPH sample (Figs. 7A and 8A) and by background spectra (Fig. 9), EPR signals caused by paramagnetic impurities in the DRs used do not constitute a problem for weak samples nor at room or at cryogenic temperatures.

4. Conclusions

Our conclusions on the present work is as follows:

- Developed DRs increase EPR signal intensity 10–170 times, depending on dielectric permittivity of its material, resonator's geometry, and sample size.
 - Resonators with $\epsilon = 160$ are twice as effective as resonators with $\epsilon = 35$.

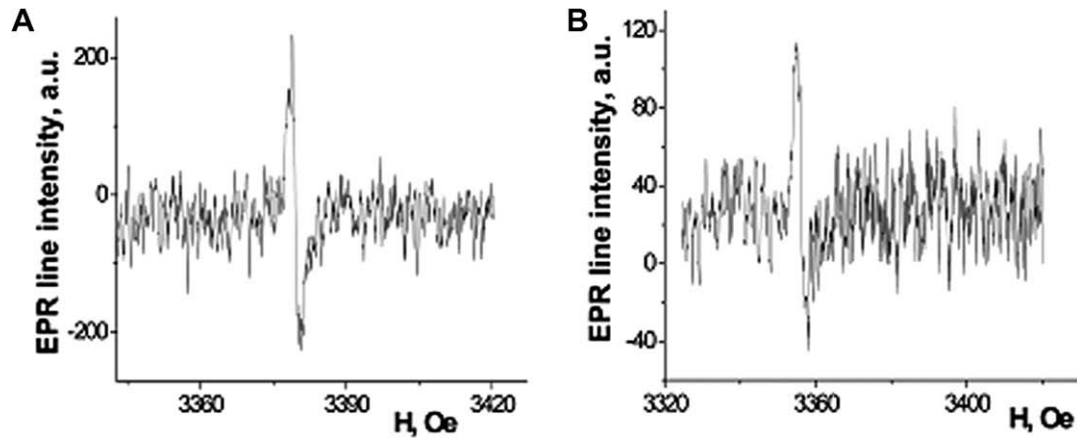


Fig. 7. EPR spectrum of a point DPPH sample (1.5×10^{13} spins/G) recorded at room temperature in DR-TE₁₀₂ structure (A) at modulation amplitude 0.125×10^{-2} Oe, $f_{\text{exp}} = 9470$ MHz and in TE₁₀₂ cavity (B) at modulation amplitude 0.125 Oe, $f_{\text{exp}} = 9410$ MHz. Other measurement conditions were identical: incident MW power 10 mW, time constant 0.3 s, scan time 60 s, without accumulation.

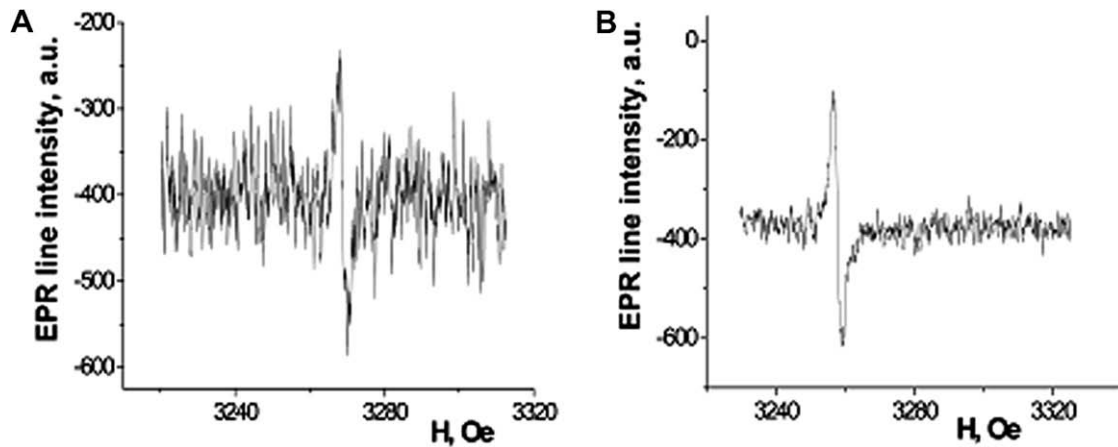


Fig. 8. EPR spectrum of a point DPPH sample (1.5×10^{13} spins/G) recorded in DR-TE₁₀₂ structure (A) at modulation amplitude 0.125×10^{-3} Oe, $f_{\text{exp}} = 9167$ MHz and in TE₁₀₂ cavity (B) at modulation amplitude 0.125×10^{-1} Oe, $f_{\text{exp}} = 9136$ MHz. Other measurement conditions were identical: $T = 77$ K, incident MW power 10 mW, time constant 0.3 s, scan time 60 s, without accumulation.

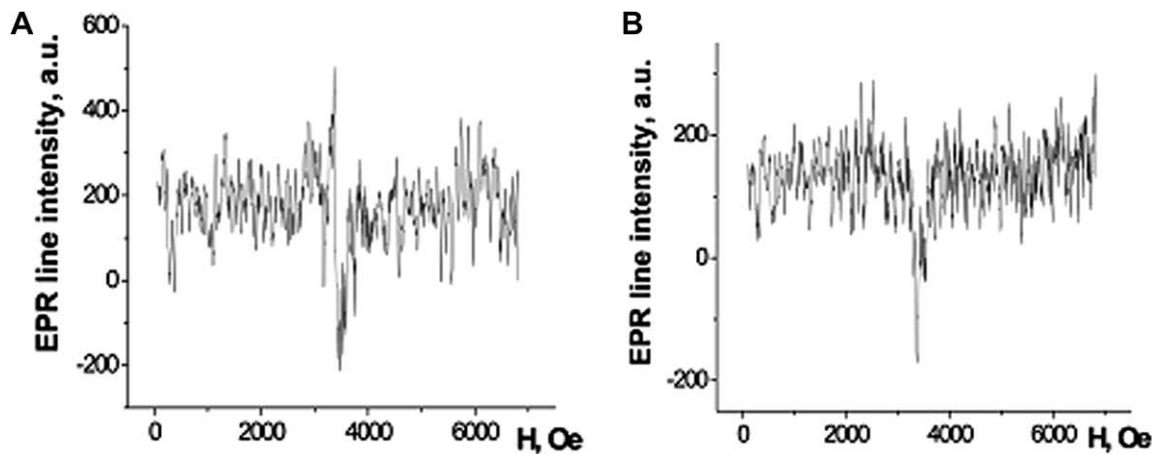


Fig. 9. The background spectra of the DR2 recorded at room (A) and liquid nitrogen (B) temperatures.

1.2. A cylindrical DR is more effective than a rectangular one (within the same value of dielectric constant of material).

1.3. The best gain in signal enhancement is achieved when the height of the sample is the same or smaller than the height of the DR used.

2. Developed resonators can be used in a wide temperature range, from 77 to 300 K.
3. A DR allows one to decrease the incident MW power by more than 100 times.

Additionally, developed DRs are promising for applications in EPR spectroscopy in two ways:

1. To increase the sensitivity of EPR spectrometers, which are now in use in radiospectroscopic laboratories, by placing a DR in the middle of a standard metallic cavity.
2. A DRs can become the basic component of portable EPR spectrometers. For example, a prototype of a portable EPR spectrometer equipped with a ferroelectric resonator made of single-crystal potassium tantalite was recently built in cooperation with EMS, Inc. company (USA) [28].

Acknowledgments

This work was supported by Grant No. UKP-5057-KV-05 from American Civilian Research and Development Foundation (CRDF) under “First Step To Market” program.

References

- [1] R.G. Saifutdinov, L.I. Larina, T.I. Vakul'skaya, M.G. Voronkov, *Electron Paramagnetic Resonance in Biochemistry and Medicine*, Kluwer Academic Publishers, New York, 2001.
- [2] F.J. Rosenbaum, Dielectric cavity resonator for ESR experiments, *Rev. Sci. Instrum.* 35 (1964) 1550–1554.
- [3] W.M. Walsh Jr., L.M. Rupp Jr., Enhanced ESR sensitivity using a dielectric resonator, *Rev. Sci. Instrum.* 57 (1986) 2278–2279.
- [4] R.W. Dykstra, G.D. Markham, A dielectric sample resonator design for enhanced sensitivity of EPR spectroscopy, *J. Magn. Reson.* 69 (1986) 350–355.
- [5] J. Wolak, B. Hilczner, Some applications of microwave ceramic ring resonator in laboratory measurements, *Ferroelectrics* 93 (1989) 73–76.
- [6] A. Sienkiewicz, K. Qu, C.P. Scholes, Dielectric resonator-based stopped-flow electron paramagnetic resonance, *Rev. Sci. Instrum.* 65 (1994) 68–74.
- [7] M. Jaworski, A. Sienkiewicz, C.P. Scholes, Double-stacked dielectric resonator for sensitive EPR measurements, *J. Magn. Reson.* 124 (1997) 87–96.
- [8] S. Del Monaco, J. Brivati, G. Gualtieri, A. Sotgiu, Dielectric resonators in a TE₁₀₂ X-band rectangular cavity, *Rev. Sci. Instrum.* 66 (1995) 5104–5105.
- [9] R. Biehl, The dielectric ring TE₀₁₁ cavity, *Bruker Rep.* 1 (1986) 45–47.
- [10] S.M. Mattar, A.H. Emwas, A tuneable doubly stacked dielectric resonator housed in an intact TE₁₀₂ cavity for electron paramagnetic resonance spectroscopy, *Chem. Phys. Lett.* 368 (2003) 724–731.
- [11] I.N. Geifman, I.S. Golovina, R.E. Zusmanov, V.I. Kofman, Raising the sensitivity of electron paramagnetic resonance spectrometer using a ferroelectric resonator, *Tech. Phys.* 45 (2000) 263–266.
- [12] Yu.E. Nesmelov, J.T. Surek, D.D. Thomas, Enhanced EPR sensitivity from a ferroelectric cavity insert, *J. Magn. Reson.* 153 (2001) 7–14.
- [13] I.N. Geifman, I.S. Golovina, Electromagnetic characterization of rectangular ferroelectric resonators, *J. Magn. Reson.* 174 (2005) 292–300.
- [14] I.N. Geifman, I.S. Golovina, Optimization of ferroelectric resonators for enhanced EPR sensitivity, *Concept Magn. Res. B* 26B (1) (2005) 46–55.
- [15] A. Blank, E. Stavitski, H. Levanon, F. Gubaydullin, Transparent miniature dielectric resonator for electron paramagnetic resonance experiments, *Rev. Sci. Instrum.* 74 (2003) 2853–2859.
- [16] I.M. Buzin, I.V. Ivanov, N.N. Moiseev, V.F. Chuprakov, Non-linearity and dielectric losses of potassium tantalite, *Fiz. Tv. Tela.* 22 (1980) 2057–2062.
- [17] I.N. Geifman, I.S. Golovina, Ferroelectric resonators for EPR spectrometers at 35, 65 and 125 GHz, in: A. Kawamori, J. Yamauchi, H. Ohta (Eds.), *EPR in the 21st Century: Basics and Applications to Material, Life and Earth Sciences*, Elsevier Science B.V., Amsterdam, 2002, pp. 694–699.
- [18] I.N. Geifman, I.S. Golovina, A. Belous, Resonance structure for EPR spectrometers. UA Patents, under pending. Application # a200706177, June 4, 2007.
- [19] A.G. Belous, O.V. Ovchar, M. Valant, D. Suvorov, Solid-state reaction mechanism for the formation of Ba_{6-x}La_{8+2x/3}Ti₁₈O₅₄ (Ln = Nd, Sm) solid solution, *J. Mater. Res.* 16 (2001) 1–7.
- [20] A.G. Belous, O.V. Ovchar, M. Valant, D. Suvorov, D. Kolar, The effect of partial isovalent substitution in the A-sublattice on MW properties of materials based on Ba_{6-x}La_{8+2x/3}Ti₁₈O₅₄ solid solutions, *J. Eur. Ceram. Soc.* 21 (2001) 2723–2730.
- [21] A. Belous, O. Ovchar, M. Valant, D. Suvorov, Abnormal behavior of the dielectric parameters of Ba_{6-x}La_{8+2x/3}Ti₁₈O₅₄ (Ln = La–Gd) solid solutions, *J. Appl. Phys.* 97 (2002) 3917–3922.
- [22] A. Belous, O. Ovchar, D. Durilin, M. Macek Krzmann, M. Valant, The homogeneity range and the microwave dielectric properties of the BaZn₂Ti₄O₁₁ ceramics, *J. Eur. Ceram. Soc.* 26 (2006) 3733–3739.
- [23] D. Kajfez, E.J. Hwan, Q-Factor measurement with network analyzer, *IEEE Trans. Microwave Theory Tech. MTT-32* (1984) 666–670; D. Kajfez, Q factor measurement, analog and digital, 1999. Available from: <www.ee.olemiss.edu/darko/rfqmeas2b.pdf>.
- [24] D.L. Griscom, R.E. Griscom, Paramagnetic resonance of Mn²⁺ in glasses and compounds of the lithium borate system, *J. Chem. Phys.* 47 (1967) 2711–2722.
- [25] J. Kreissl, W. Gehlhoff, EPR investigations of ZnS:Mn and ZnSe:Mn, *Phys. Stat. Sol. (A)* 81 (1984) 701–707.
- [26] A. Blank, J.H. Freed, N.P. Kumar, C.H. Wang, Electron spin resonance microscopy applied to the study of controlled drug release, *J. Control. Release* 111 (2006) 174–184.
- [27] C.P. Poole Jr., *Electron Spin Resonance: A Comprehensive Treatise on Experimental Techniques*, second ed., Dover, Mineola, NY, 1996.
- [28] I.N. Geifman, I.S. Golovina, Magnetic resonance spectrometer, US Patent 7,268,549B2, September 11, 2007.